Journal of Physiology (1992), **448**, *pp.* 99–119
With 12 figures
Printed in Great Britain

ACTIONS OF PERCHLORATE IONS ON RAT SOLEUS MUSCLE FIBRES

By ANGELA F. DULHUNTY, PEI-HONG ZHU*, MICHAEL F. PATTERSON AND GERARD AHERN†

From the Muscle Research Group, JCSMR, Australian National University, PO Box 334, Canberra, ACT 2601, Australia

(*Received 18 March 1991*)

SUMMARY

1. The effects of perchlorate (ClO_4^-) on contraction have been studied in rat soleus muscle fibres using (i) potassium (K^+) contracture and (ii) two-microelectrode-point voltage clamp techniques.

2. Membrane potentials (V_m) at all external [K^+] were 3–5 mV more negative in ClO_4^-. The hyperpolarization could not be attributed to a change in Na^+, K^+, or Cl^- permeability, or to an effect on the Na^+–K^+ pump.

3. ClO_4^- shifts the voltage dependence of tension activation, and contraction threshold, to more negative membrane potentials without altering maximum tension. Consequently, twitches and submaximal K^+ contractures were potentiated, whereas tetanic contractions and 200 mM-K^+ contractures were unaltered.

4. The decay of K^+ contractures during steady depolarization with ClO_4^- developed a slow exponential phase with an average time constant of $6{\cdot}05 \pm 0{\cdot}76$ min at -38 mV, and $1{\cdot}68 \pm 0{\cdot}15$ min at -19 mV. This slow component was (a) under the rapid control of the surface V_m and (b) did not depend on external Ca^{2+}.

5. Inactivation of E–C coupling was measured with a test 200 mM-K^+ depolarization following 3–10 min depolarizations in conditioning solutions containing 20–120 mM-K^+. ClO_4^- induced a negative shift in the curve-relating test K^+ contracture amplitude to conditioning V_m but did not alter the rate of repriming of tension upon repolarization.

6. The results suggest that ClO_4^- increases the amount of activator produced during depolarization and thus allows the slow inactivation step in excitation–contraction (E–C) coupling to be reflected in the decay of K^+ contracture tension.

7. A 'perchlorate contracture', which did not depend on the activation of E–C coupling, was observed. The contracture depended on external Ca^{2+}, but not on voltage-dependent Ca^{2+} channels or Na^+–Ca^{2+} exchange.

* Present address: Shanghai Institute of Physiology, Chinese Academy of Sciences, 320 Yue Yang Road, Shanghai, China.

† Present address: Department of Zoology, University of Canterbury, Christchurch 1, New Zealand.

MS 9241

INTRODUCTION

The aim of the experiments was to examine the effects of perchlorate ions (ClO_4^-) on excitation–contraction (E–C) coupling in rat soleus muscle fibres. Both the activation and inactivation processes that characterize E–C coupling in skeletal muscle are thought to depend on conformational states of a voltage-sensitive molecule in the T-tubule membrane (Chandler, Rakowski & Schneider, 1976). ClO_4^- shifts the activation of tension to more negative membrane potentials in amphibia, but has little effect on inactivation (Foulks, Miller & Perry, 1973; Foulks & Perry, 1979; Gomolla, Gottschalk & Luttgau, 1983; Luttgau, Gottschalk, Kovacs & Fuxreiter, 1983). The primary action of ClO_4^- is on the voltage-sensitive molecule since it causes the same negative shift in the activation of asymmetric charge movement (Luttgau *et al.* 1983; Huang, 1986; Csernoch, Kovacs & Szucs, 1987). ClO_4^- is a chaotropic anion that induces a 'surface charge' on lipid bilayer membranes (McLaughlin, Bruder, Chen & Moser, 1975). These properties cannot explain its effect on muscle since voltage-dependent Na^+ and K^+ conductances are not altered (Gomolla *et al.* 1983).

ClO_4^- has proved useful in investigations of the inactivation process in mammals. The onset of steady-state inactivation, during prolonged depolarization in high external K^+ concentrations, follows a biphasic time course thought to reflect the transitions to two inactivated conformations of the voltage-sensitive molecule (Dulhunty, 1991). The possibility that the voltage sensor can assume two inactivated states has also been considered to explain results obtained in frog muscle (Luttgau, Gottschalk & Berwe, 1986; Berwe, Gottschalk & Luttgau, 1987). However, if there are two inactivated states in E–C coupling, it is curious that the transition to the second state is not reflected in the decline of K^+ contractures during maintained depolarization (Hodgkin & Horowicz, 1960; Luttgau, 1963). K^+ contracture tension in rat soleus fibres declines with the same time course as the fast phase in the development of steady-state inactivation (Dulhunty, 1991). It will be shown in this report that ClO_4^- 'unmasks' a slow component in the decay of K^+ contracture tension which follows the slow component of steady-state inactivation.

In addition to its effect on the decay of K^+ contracture tension, ClO_4^- produced the usual shift in the activation curve to more negative potentials (Foulks *et al.* 1973; Foulks & Perry, 1979; Gomolla *et al.* 1983; Luttgau *et al.* 1983) and, unexpectedly, induced a negative shift in the steady-state inactivation curve. Furthermore, ClO_4^- hyperpolarized the muscle fibres and induced a contracture at the resting membrane potential.

METHODS

The methods used have been previously described in detail (Dulhunty, 1991). A brief summary follows.

Biological preparation and solutions. Adult male Wistar rats were asphyxiated in CO_2 and soleus muscles removed for dissection into bundles of five to ten fibres. Standard control and high-K^+ solutions are given in Dulhunty (1991). Other solutions are listed in Table 1. High-K^+ solutions are referred to by the $[K^+]$ (in mM): for example, contractures in 200 mM-K^+ are referred to as 200 mM-K^+ contractures. ClO_4^- was added as $NaClO_4$. The experiments were performed at $22{\cdot}5 \pm 0{\cdot}5$ °C.

Isometric tension recording. Fibres were attached to an Akers transducer (model AE875, SensoNor a.s. Horten, Norway) mounted in a 0·5 ml rapid-flow (2 ml/s) bath (equilibration time

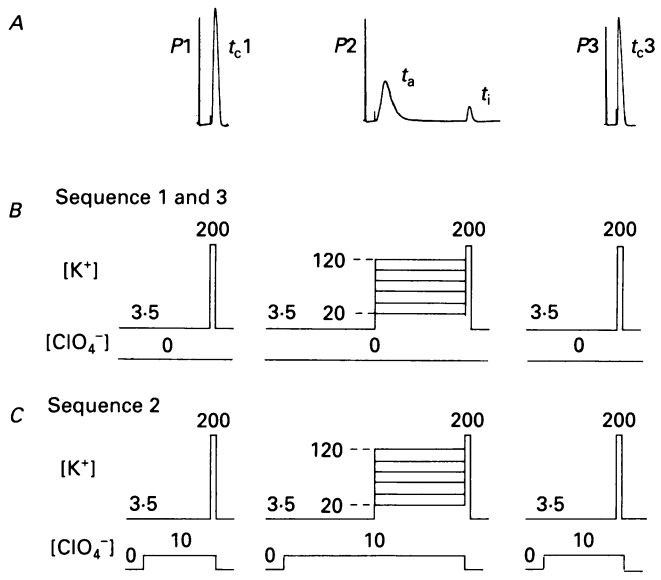

Fig. 1. Two-pulse protocol used to measure the activation and inactivation of K^+ contracture tension. The records in *A* show a control sequence of tetanic contractions and K^+ contractures. The symbols are defined in the text. K^+ contractures, t_c1, t_i and t_c2, were evoked by depolarization in 200 mM-K^+, while the conditioning K^+ contracture (t_a) was elicited by exposure to 60 mM-K^+. The solution changes are illustrated in *B* where $[K^+]$ is in mM and conditioning $[K^+]$ varied from 20 to 120 mM. *C* shows the solution changes in the presence of ClO_4^-. $[ClO_4^-]$ is in mM.

TABLE 1. Solutions other than those listed in Table 1 of Dulhunty (1991)

A. Low-calcium series

Solution	Na_2SO_4	NaCl	K_2SO_4	KCl	$CaSO_4$	$MgSO_4$	$CoSO_4$	Sucrose	CaEGTA	TES
				Low-calcium, 10 mM-$MgSO_4$ solutions						
A Control	32·25	16	1·75	0	0	10	0	100	20	10
B 40 mM-K^+	80	0	12	16	0	10	0	0	20	10
				Low-calcium, 10 mM-$CoSO_4$ solutions						
C Control	32·25	16	1·75	0	0	0	10	170	0	2
D 40 mM-K^+	80	0	12	16	0	0	10	0	0	2

B. Low-sodium and zero-chloride series

Solution	Na_2SO_4	NaCl	$LiSO_4$	K_2SO_4	KCl	$CaSO_4$	$MgSO_4$	Sucrose	TES
				Low-sodium, $LiSO_4$ solutions					
E Control	0	16	32·25	1·75	0	7·6	1	170	2
F 40 mM-K^+	16	0	64	12	16	7·6	1	170	2
				Zero-sodium, $LiSO_4$ solutions					
G control	0	0	48	1·75	0	7·6	1	170	2
H 40 mM-K^+	0	0	80	12	16	7·6	1	170	2
				Zero-chloride					
I Control	48	0	0	1·75	0	7·6	1	170	2

Concentrations are in mM. All solutions contained 11 mM-glucose. TES, *N*-tris-(hydroxymethyl)-methyl-2-amino-ethanesulphonic acid) buffer. pH was adjusted to 7·4 with NaOH.

< 0·5 s). Tension was recorded on a chart recorder (7402A, Hewlett-Packard Co., Palo Alto, CA, USA) and selected responses stored on magnetic disc for computer analysis.

Data analysis and normalization. The voltage dependence of activation and inactivation of tension was determined using peak amplitudes of the seven tetanic and K^+ contracture responses shown in Fig. 1*A*. The symbols are fully defined in Dulhunty (1991). The seven responses were:

(1) a tetanus in 3·5 mM-K^+ ($P1$)
(2) a control 200 mM-K^+ contracture (t_c1)
(3) a recovered tetanus in 3·5 mM-K^+ ($P2$)
(4) a conditioning K^+ contracture (t_a, used to construct *activation* curves)
(5) a test 200 mM-K^+ contracture (t_i, used to construct *inactivation* curves)
(6) a recovered tetanus in 3·5 mM-K^+ ($P3$)
(7) a control 200 mM-K^+ contracture (t_c3).

Two sequences, performed in ClO_4^--free solutions (1 and 3, Fig. 1*B*), bracketed a sequence (2, Fig. 1*C*) in which fibres were exposed to ClO_4^- for 3–5 min before each K^+ contracture (i.e. t_c1, t_a+t_i or t_c3). The fibres recovered in control solutions for 10–15 min after each session in ClO_4^- and high $[K^+]$.

The following normalization procedures avoided assumptions about the time course of 'run-down'. The amplitudes of t_c1, t_a, t_i and t_c3 were divided by the amplitude of the preceding tetanus ($P1$, $P2$ or $P3$) and then normalized to T_{max}, the mean amplitude of control 200 mM-K^+ contractures,

$$T_{max} = (t_c1/P1 + t_c3/P3)/2. \quad (1)$$

Conditioning K^+ contracture tension, T_a, was given by

$$T_a = (t_a/P2)T_{max}, \quad (2)$$

and test 200 mM-K^+ contracture tension, T_i, was given by

$$T_i = [(t_i - t_p)/P2]/T_{max}, \quad (3)$$

where t_p, the residual pedestal tension, was subtracted from t_i to yield a tension produced by additional depolarization in 200 mM-K^+. In ClO_4^- sequences, K^+ contracture tension was normalized to the tetanus recorded immediately before exposure to ClO_4^- (see Fig. 2*A*, *B* and *C* below).

Construction of activation and inactivation curves. T_a was plotted against membrane potential, V_m (Table 2),and an activation curve obtained by fitting a Boltzmann equation of the form:

$$T_a = T_{max}/[1 + \exp(V_a - V_m)K_a], \quad (4)$$

where V_a is the V_m at which $T_a = 0{\cdot}5T_{max}$ and K_a is a slope factor.
Inactivation curves, at time t, were obtained from a graph of $T_{i(t)}$ against conditioning membrane potential, V_c. The data were fitted with a Boltzmann equation of the form:

$$T_{i(t)} = T_{max}/[1 + \exp(V_c - V_{i(t)})/k_{i(t)}] \quad (5)$$

where $V_{i(t)}$ is the V_c at which $T_{i(t)} = 0{\cdot}5\ T_{max}$ and $k_{i(t)}$ is a slope factor.

Intracellular microelectrodes. Glass microelectrodes were filled with 2·5 M-KCl (2–5 MΩ). V_m was measured as the difference between an intracellular voltage and an external reference microelectrode.

Two-microelectrode voltage clamp. The technique (Chua & Dulhunty, 1988), was based of that on Adrian, Chandler & Hodgkin (1969) and Costantin (1974). Current and voltage electrodes were inserted at opposite edges of a fibre and surface sarcomeres between the electrodes displayed on a videomonitor via a video camera (800 lines/in) attached to a Zeiss microscope with an Olympus 6·0 mm working distance 32× air objective and 16× Zeiss eyepiece. Tetrodotoxin, 2×10^{-7} M, in the bathing solution prevented action potentials. Fibres were held at −80 mV. Depolarizing pulses, applied every second, were increased in 2 mV steps until movement was detected and then reduced in 0·2 mV steps to a potential that no longer produced visible movement, the 'threshold potential'.

RESULTS

ClO_4^- induced hyperpolarization

Intracellular membrane potentials were measured to provide data necessary for subsequent sections in which tension parameters are plotted as a function of V_m.

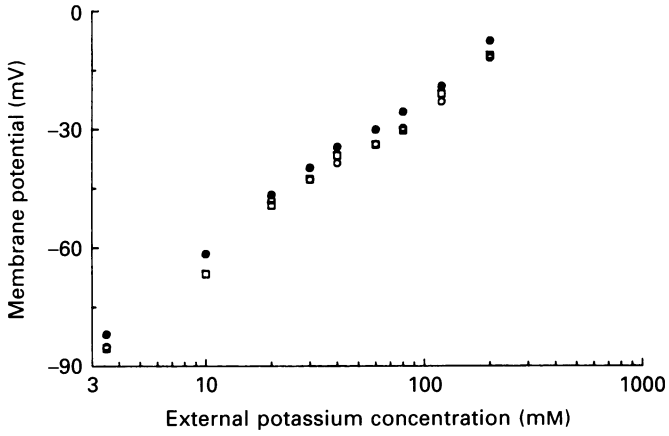

Fig. 2. The effect of ClO_4^- on the relationship between intracellular membrane potential and external $[K^+]$. ●, control data; ○, data in 2 mM-ClO_4^-; □, data in 10 mM-ClO_4^-. Each point is the average membrane potential obtained in at least ten fibres. Standard error bars are within the dimensions of the symbols.

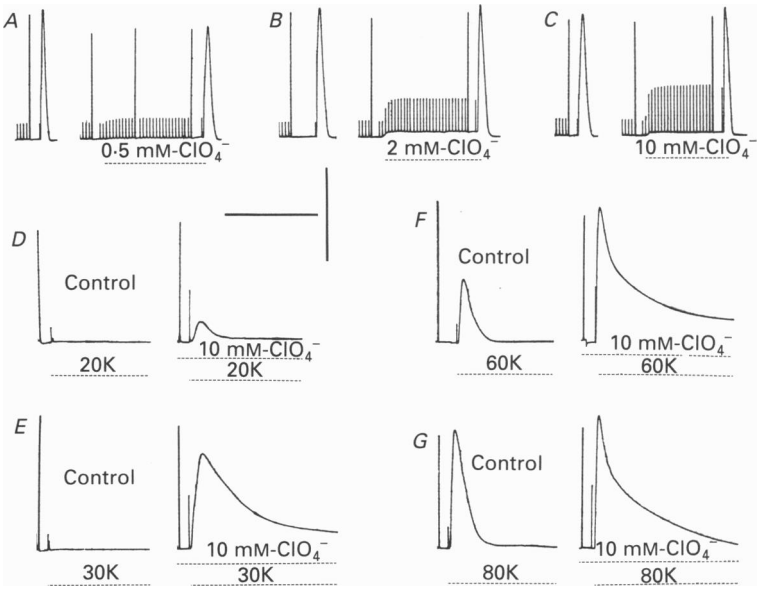

Fig. 3. The effect of ClO_4^- on twitch (small vertical deflections), tetanus (large vertical deflections) and K^+ contracture (slower transients) tension. The dotted lines indicate exposure to ClO_4^- or to high-K^+ solutions. *A*, *B* and *C* show exposures to 0·5, 2 and 10 mM ClO_4^-. The first pair of records was obtained in control solutions and the second pair recorded after recovery from 200 mM-K^+ and during exposure to ClO_4^-. 200 mM-K^+ was washed out of the bath at the peak of each 200 mM-K^+ contracture. *D*, *E*, *F* and *G* show the effect of 10 mM-ClO_4^- on 20, 30, 60 and 80 mM-K^+ contractures. Horizontal calibration, 5 min. The vertical calibration, in mN, was the same in each pair of records and varied between 4 and 8 mN.

Membrane potentials in ClO_4^- (2 or 10 mM) were 2–5 mV more negative than normal, although the usual logarithmic relationship between $[K^+]$ and V_m remained (Fig. 2). A hyperpolarization of resting membrane potentials has also been reported

in amphibia (Gomolla *et al.* 1983). The effect on membrane potential was not due to a change in Cl^- permeability or the Na^+–K^+ pump since average hyperpolarizations of $-2{\cdot}5 \pm 0{\cdot}04$ mV ($n = 41$) and $-2{\cdot}6 \pm 0{\cdot}09$ mV ($n = 22$) were recorded respectively in zero Cl^- and after 3 h in 1 mM-ouabain.

ClO_4^- potentiates twitches but not maximum tension

An increase in twitch tension followed addition of ClO_4^- to the bathing solution (Fig. 3) and was complete within 30 s, the time required for small ions to equilibrate

TABLE 2. Effect of ClO_4^- at 0·5, 2 and 10 mM on the twitch-to-tetanus ratio, peak tetanic tension and the amplitude of 200 mM-K^+ contractures

	Twitch-to-tetanus ratio	Relative tetanic tension	200 mM-K^+ contracture tension	
			Normalized to control tetanus	Normalized to tetanus in ClO_4^-
Control	0·11 ± 0·01 (16)	1·00 (16)	1·11 ± 0·19 (5)	
500 μM-ClO_4^-	0·14 ± 0·01 (16)	1·02 ± 0·17 (16)	1·11 ± 0·19 (5)	1·07 ± 0·19 (5)
Control	0·11 ± 0·01 (68)	1·00 (68)	0·99 ± 0·02 (68)	
2 mM-ClO_4^-	0·23 ± 0·01 (68)	1·06 ± 0·01 (68)	1·11 ± 0·03 (68)	1·03 ± 0·03 (68)
Control	0·12 ± 0·01 (31)	1·00 (31)	1·02 ± 0·02 (31)	
10 mM-ClO_4^-	0·38 ± 0·01 (31)	1·04 ± 0·01 (31)	1·16 ± 0·03 (31)	1·02 ± 0·01 (31)

The data are shown as means ± 1 S.E.M., with the number of fibres in parentheses.

in mammalian T-tubules (Dulhunty, 1979). Twitch amplitude, and twitch-to-tetanus ratio, increased further in 10 mM-ClO_4^- than in 0·5 or 5 mM (Table 2). Maximum tension, reflected in peak tetanic and 200 mM-K^+ contracture tension (Dulhunty & Gage, 1985), was relatively insensitive to ClO_4^- (Fig. 3 and Table 2).

An increase in resting tension was seen with 2 or 10 mM-ClO_4^- (Fig. 3). This novel 'ClO_4^- contracture' is discussed in a later section.

Effects of ClO_4^- on submaximal K^+ contractures and activation

ClO_4^- potentiated submaximal K^+ contracture tension (Fig. 3*D–G*) and, surprisingly, prolonged the decay of tension (see following sections). The potential for 50% activation was shifted by -10 mV in 2 mM-ClO_4^- and by -15 mV in 10 mM-ClO_4^- (Fig. 4 and Table 3). However, there was no change in the slope of the curves. Rat fibres were less sensitive to ClO_4^- than voltage-clamped frog fibres where 8 mM-ClO_4^- produced a -25 mV shift in activation (Gomolla *et al.* 1983; Luttgau *et al.* 1983). To determine whether the difference was due to the use of voltage clamp as opposed to K^+ contractures, contraction thresholds were measured using a two-microelectrode-point voltage clamp.

An average control membrane potential for contraction threshold of $-45 \pm 0{\cdot}6$ mV for a 500 ms test pulse agreed with the K^+ contracture (Fig. 4*A*). Thresholds for 5–100 ms test pulses were more negative by 7 or 8 mV with 2 mM-ClO_4^-, or 12–15 mV with 10 mM-ClO_4^- (Fig. 4*B*). These changes in threshold confirm the shifts in V_a (Table 3), since k_a did not change in ClO_4^-.

Strength–duration curves reflect the kinetics of Ca^{2+} release from the sarcoplasmic reticulum (Adrian *et al.* 1969; Costantin, 1974). The parallel shift in the curve for

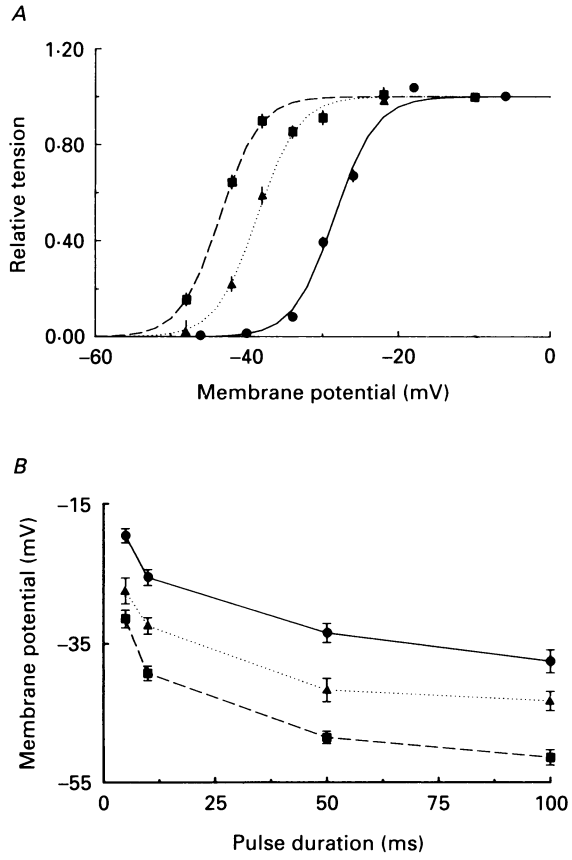

Fig. 4. The effect of ClO_4^- on the activation of contraction. Relative K^+ contracture tension, T_a (eqn (2), Methods), is plotted against V_m measured in high-K^+ solutions (Fig. 2) in *A*. The symbols show average results obtained in control solutions (●, $n = 15$), 2 mM-ClO_4^- (▲, $n = 10$) and 10 mM-ClO_4^- (■, $n = 5$). The membrane potential at contraction threshold, measured under two-microelectrode-point voltage clamp conditions, is plotted against test pulse duration in *B*. Average results are shown for fibres in control solutions (●, $n = 19$), 2 mM-ClO_4^- (▲) $n = 10$) and 10 mM-ClO_4^- (■, $n = 13$). The vertical bars indicate ±S.E.M. where this is greater than the dimensions of the symbols.

TABLE 3. Effects of ClO_4^- on V_a and k obtained from the best, least-squares fit of eqn (4) to the average, normalized K^+ contracture data

	T_{max}	V_a (mV)	k (mV)
Control	1·00	−28·4	2·7
2 mM-ClO_4^-	1·00	−38·6	2·7
10 mM-ClO_4^-	1·00	−43·5	2·6

pulse durations between 10 and 100 ms (Fig. 4*B*) suggests that ClO_4^- did not alter the rate of Ca^{2+} release.

Perchlorate 'unmasks' a slow component in K^+ contractures

The slow decay of K^+ contractures in ClO_4^- (Fig. 5*A*) was surprising since it is not seen in frog fibres (Gomolla *et al.* 1983) and inactivation is faster at more depolarized

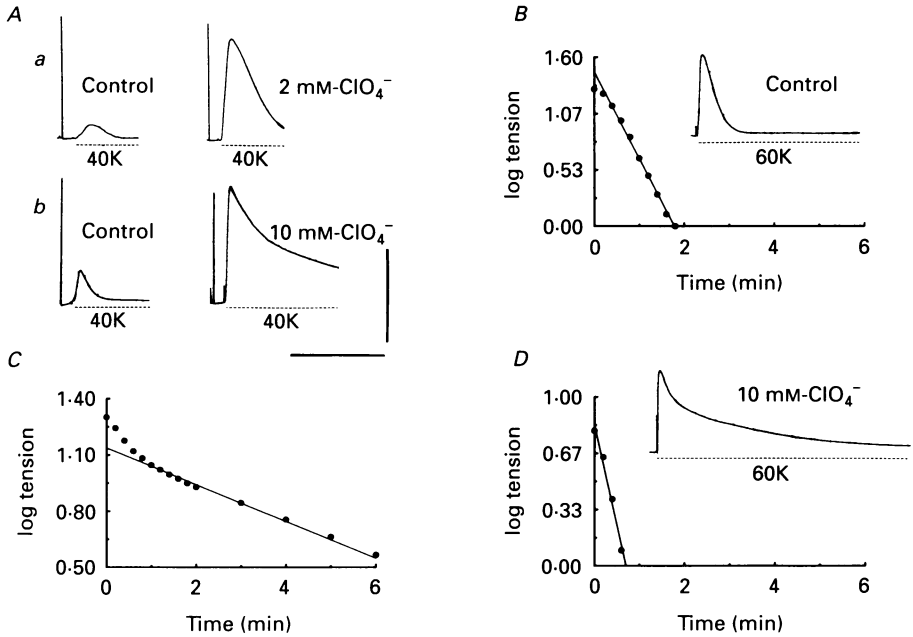

Fig. 5. The effect of ClO_4^- on the decay of K^+ contractures. *A*, 40 mM-K^+ contractures in control solutions and 2 mM-ClO_4^- (*a*) or 10 mM-ClO_4^- (*b*). Horizontal calibration, 5 min; vertical calibration, 3 mN for *A a* and 6 mN for *A b*. *B*, *C* and *D* are graphs of log tension *vs.* time. *B*, decay of a control 60 mM-K^+ contracture (shown as the inset in *B*): the line through the data ($r^2 = 0{\cdot}996$) has a time constant 0·53 min. *C*, 60 mM-K^+ contracture in 10 mM-ClO_4^- (shown as the inset in *D*): the line through the slow component of the contracture, between 1 and 6 min ($r^2 = 0{\cdot}999$), has a time constant of 4·5 min. The slow component was subtracted from the full decay of the K^+ contracture in 10 mM-ClO_4^- to obtain the points plotted in *D*: the line through the points ($r^2 = 0{\cdot}9825$) has a time constant of 0·38 min.

V_m (Hodgkin & Horowicz, 1960). We expected that, if ClO_4^- had an effect, tension might fall more rapidly with enhanced activation.

Analysis of the effect of ClO_4^- on K^+ contracture decay

The decay of control K^+ contractures, after the first 10 s, was exponential (Fig. 5*B*). The initial S-shaped decay was less than the exponential prediction. The decay in 10 mM-ClO_4^- could be fitted by the sum of two exponentials (Fig. 5*C* and *D*). The time constants obtained from exponential curves fitted to the decay of K^+ contractures (with average r^2 values greater than 0·9562) were voltage dependent in both control (Fig. 6*A*) and 10 mM-ClO_4^- solutions Fig. 6*A* and *B*).

The initial decay of tension was similar in control solutions and in ClO_4^- when records were scaled to the same peak amplitude and superimposed (Fig. 6*C* and 6*D*). The time taken for tension to fall from the peak to 90% of peak tension was also voltage dependent and was, on average, slightly faster in ClO_4^- than in normal solutions (Fig. 6*E*).

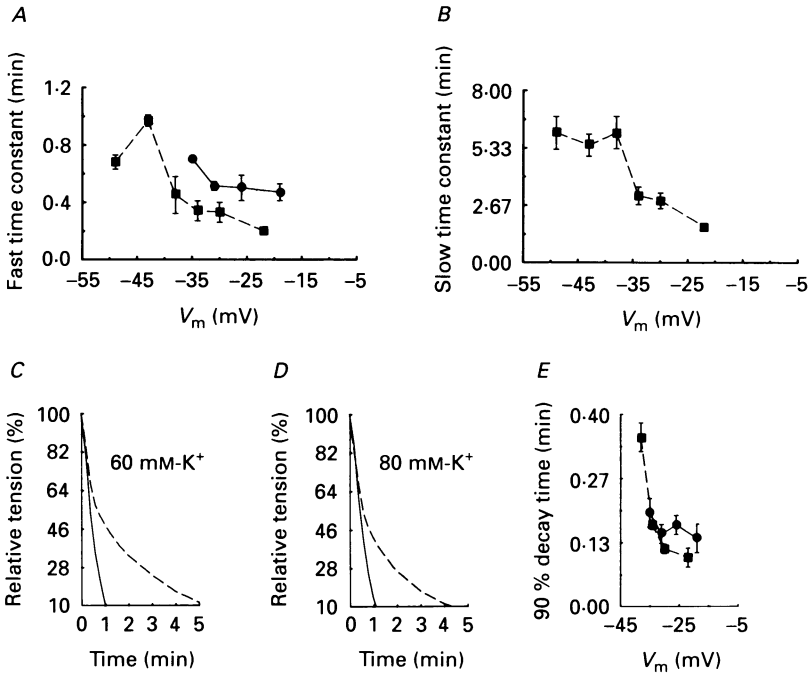

Fig. 6. *A* and *B* show average time constants of decay of K^+ contractures at different membrane potentials (Table 2). *A*, control time constants (●) and fast time constants in 10 mM-ClO_4^- (■). *B*, slow time constants in 10 mM-ClO_4^- (■). *C* and *D*, superimposed decays of K^+ contractures in control solutions (continuous lines) and 10 mM-ClO_4^- (dashed lines), scaled to the same peak tension. Each pair of records was obtained from one preparation. *E*, 90% decay time: average control data (●) and average data with 10 mM-ClO_4^- (■) are shown. Vertical bars indicate ±S.E.M. where this exceeds the dimensions of the symbols.

The origin of the slow component in K^+ contracture tension

An exciting possibility was that ClO_4^- unmasked the slow phase of inactivation in the decay of K^+ contracture tension (see Introduction). However it was equally possible that ClO_4^- prolonged the tension transient by activating Ca^{2+} release from the sarcoplasmic reticulum through some separate mechanism. The following questions were addressed therefore.

The influence of voltage-dependent Ca^{2+} channels?

The voltage dependence of the slow decay of tension suggested that it was generated by processes in the surface/T-tubule membrane. Ca^{2+} entry through voltage-activated Ca^{2+} channels in the T-system (Siri, Sanchez & Stefani, 1980;

Almers, McCleskey & Palade, 1985) can be eliminated by low external [Ca^{2+}] or by Ca^{2+} channel blockers. External Ca^{2+} was replaced by 10 mM-Mg^{2+} or 10 mM-Co^{2+} (Table 1), in solutions with measured [Ca^{2+}] of 85 and 15 μM, respectively (Dulhunty & Gage, 1988). The Mg^{2+} solution contained 20 mM-CaEGTA. Co^{2+} replaced external

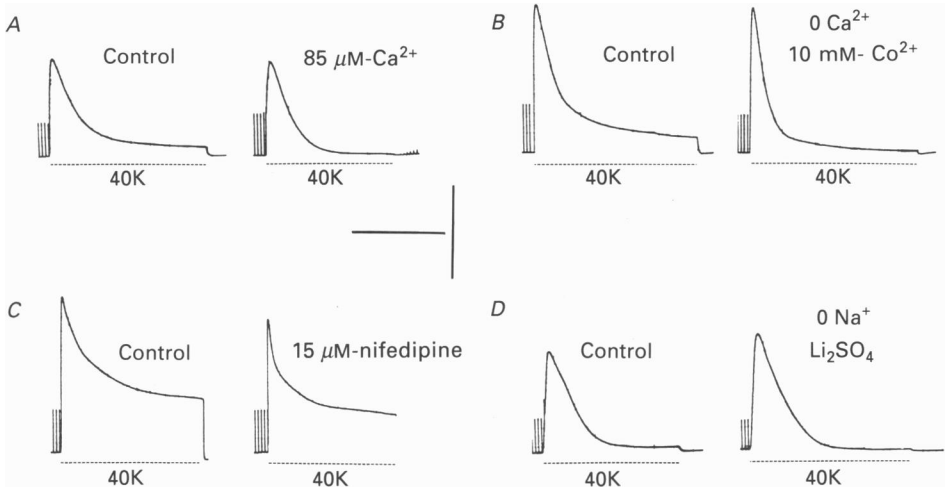

Fig. 7. 40 mM-K^+ contractures in 10 mM-ClO_4^-. Control records were obtained after a 5 min incubation in 10 mM-ClO_4^-. Test records were obtained using test 40 mM-K^+ solutions (Table 1) after 10–15 min incubation in the test 3·5 mM-K^+ solution followed by a 5 min incubation in test 3·5 mM-K^+ solution plus 10 mM-ClO_4^-. Each pair of records was from one preparation. Test procedures are indicated beside each test record. Analyses of the records is presented in Tables 4–6. *A*, series 1, data set 1, C2 (Table 4). *B*, series 2, data set 1, C1 (Table 4). *C*, series 1, data set 1, C1 (Table 5). *D*, series 1, data set 2, C1, (Table 6). Calibrations: horizontal, 5 min; vertical, 8 mN for *A*, 5 mN for *B* and *C*, 6 mN for *D*.

Ca^{2+} and blocked the Ca^{2+} channel (Almers *et al.* 1985). Although the slow time constant became faster in both solutions (Fig. 7*A* and *B*, Table 4), the amplitude of K^+ contractures was not reduced (Table 4). The Ca^{2+} channel blocker nifedipine (Almers *et al.* 1985), at 15 or 50 μM, had no effect on the amplitude or decay of K^+ contractures in ClO_4^- (Fig. 7*C* and Table 5).

These experimental manipulations suggested that external Ca^{2+} might modulate the kinetics of K^+ contracture decay but that tension was not maintained by Ca^{2+} influx through dihydropyridine-sensitive, voltage-dependent, Ca^{2+} channels.

The influence of Na^+–Ca^{2+} exchange

Ca^{2+} entering depolarized fibres via the Ca^{2+}–Ca^{2+} exchange mode of the Na^+–Ca^{2+} exchange protein (Philipson, 1985) might contribute to K^+ contractures (Curtis, 1988; Noireaud & Leoty, 1988). Although external [Ca^{2+}] was previously reduced to 15 μM, the [Ca^{2+}] in the T-system might have been higher and Ca^{2+} may have entered through Ca^{2+}–Ca^{2+} exchange. Replacement of external Na^+ with Li^+stimulates Ca^{2+}–Ca^{2+} exchange (Baker, Blaustein, Hodgkin & Steinhardt, 1967; Blaustein & Hodgkin, 1969). K^+ contractures in ClO_4^- were not potentiated in Li^+

solutions (Fig. 7*D*, Table 6) suggesting that tension was independent of Ca^{2+}–Ca^{2+} exchange.

Do K^+ contractures depend on any slow secondary process?

ClO_4^- may have induced a second messenger such as inositol 1,4,5-trisphosphate ($InsP_3$) which stimulates Ca^{2+} release from the sarcoplasmic reticulum (Vergara,

TABLE 4. The effect of low external [Ca^{2+}] on the amplitude and decay of 40 mM-K^+ contractures in 10 mM-ClO_4^-

Data set	K^+ contracture	Relative peak tension (%)	Fast time constant (min)	Slow time constant (min)	Fraction of peak tension contained in the slow component (%)
Series 1: 10 mM-Mg^{2+}, 20 mM-CaEGTA (85 μM-(Ca^{2+}) (solutions A and B, Table 1)					
1	C1	100	1·42	3·9	26
	T	80	0·57	2·5	5
	C2	82	1·21	2·0	75
2	C1	100	0·72	4·6	29
	T	100	0·73	1·8	12
	C2	100	0·72	3·6	25
Series 2: 10 mM-Co^{2+} (15 μM-Ca^{2+}) (solutions C and D, Table 1)					
1	C1	100	0·62	3·9	56
	T	89	0·39	2·5	5
	C2	86	0·47	2·0	75
2	C1	100	—	1·3	100
	T	84	0·19	—	0
	C2	108	0·41	1·7	45

The first K^+ contracture (C1) was elicited in Ca^{2+}-containing solutions, the second, (T), in low-Ca^{2+} solutions and the third (C2) after recovery in control [Ca^{2+}]. Each set of data (1, 2 etc.) was obtained from one preparation. Peak tension (column 1), relative to C1, provides an index of run-down in tension during the experiment. The amplitude of contractures was measured from the peak to the completion of the decay, either the baseline or to a pedestal tension. Time constants (columns 2 and 3) were determined from exponential curves fitted to the decay of K^+ contractures (average r^2 values for each preparation were greater than 0·980). Column 4 shows the fraction of tension attributed to the slow component of the K^+ contracture (determined by extrapolation of the slow exponential component to zero time).

Tsien & Delay, 1985; Volpe, Salviati, Di Virgilio & Pozzan, 1985). Since Li^+ interferes with inositol metabolism (Berridge & Irvine, 1989) the lack of a Li^+ effect (above) suggests that $InsP_3$ is not involved. The rapid decay of K^+ contracture tension upon repolarization (Fig. 7*C*) was similar to that seen after brief depolarizations in the absence of ClO_4^- (Dulhunty, 1991) and suggested that tension was not maintained by a slow secondary process. Tension during the entire K^+ contracture was under the rapid control of T-tubule membrane potential and normal voltage activation processes.

The results support the suggestion that the slow phase of decay of K^+ contracture tension in ClO_4^- reflects a slow phase in the inactivation of E–C coupling.

TABLE 5. The effect of 15 and 50 μM-nifedipine on the amplitude and decay of 40 mM-K^+ contractures in 10 mM-ClO_4^-

Data set	K^+ contracture	Relative peak tension (%)	Fast time constant (min)	Slow time constant (min)	Fraction of peak tension contained in the slow component (%)
		Series 1: 15 μM-nifedipine			
1	C1	100	0·78	1·6	20
	T	85	0·70	1·8	8
	C2	80	0·53	1·9	9
2	C1	100	0·82	3·3	33
	T	93	0·60	3·6	34
	C2	78	0·58	3·4	16
		Series 2: 50 μM-nifedipine			
1	C1	100	0·47	3·6	36
	T	98	0·65	1·8	36
	C2	—	—	—	—
2	C1	100	0·58	2·9	100
	T	90	0·19	—	0
	C2	82	0·41	—	0

The first K^+ contracture, (C1), was elicited in the absence of nifedipine, the second (T) after 10 min equilibration in the nifedipine-containing solution and the third, (C2), after recovery from nifedipine. The contents of each column are as described for Table 4 (average r^2 values for each preparation were greater than 0·980). Nifedipine was dissolved in ethanol at a stock concentration of 10 mM, and then added to the control solution (Table 1, Dulhunty, 1991) to give final concentrations of 15 or 50 μM.

TABLE 6. The effect of replacement of Na^+ with Li^+ on the amplitude and decay of 40 mM-K^+ contractures in 10 mM-ClO_4^-

Data set	K^+ contracture	Relative peak tension (%)	Fast time constant (min)	Slow time constant (min)	Fraction of peak tension contained in the slow component (%)
		Series 1: 16 mM-Na^+, 64 mM-Li_2SO_4 (solutions E and F, Table 1)			
1	C1	100	—	3·0	100
	T	69	1·20	3·4	12
	C2	58	0·80	4·1	10
		Series 2: 0 mM-Na^+, 80 mM-Li_2SO_4 (solutions E and F, Table 1)			
1	C1	100	0·82	4·8	46
	T	86	0·60	3·7	32
	C2	77	0·58	5·6	8
2	C1	100	—	4·0	100
	T	71	0·72	3·1	31
	C2	68	0·80	3·7	16

The first K^+ contracture was elicited by the Na_2SO_4 solution (C1), the second (T) after 15 min to 20 min in Li_2SO_4 (solutions E, F, G and H, Table 1) and the third after recovery in Na_2SO_4 (C2). The columns are as described for Table 4 (average r^2 values for each preparation were greater than 0·980).

Effects of ClO_4^- on the activation of maximum tension

The amplitude of test 200 mM-K^+ contractures, normally equivalent to tetanic tensions (Figs 1 and 3 above), was smaller than the tetanus after conditioning depolarizations in high K^+ and was depressed further in the presence of 10 mM-ClO_4^-

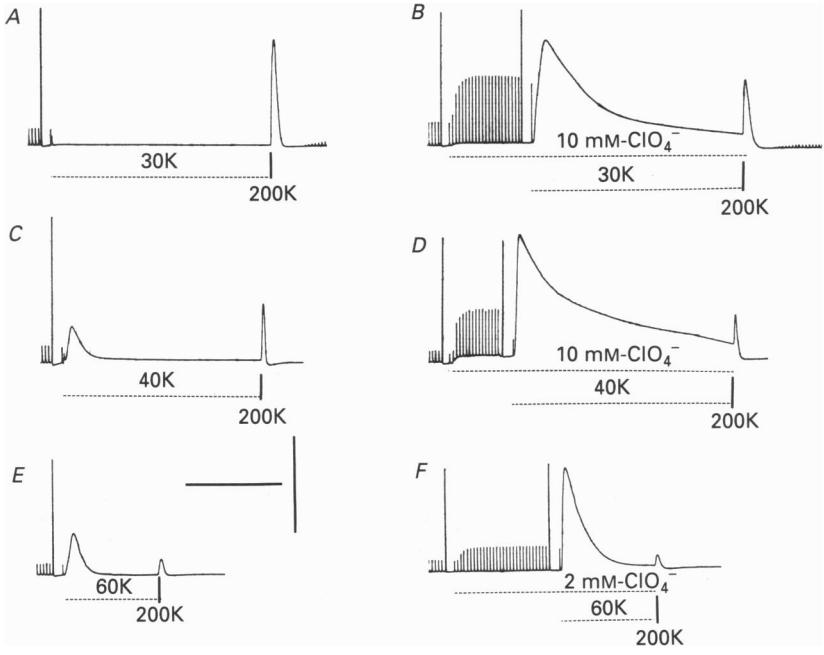

Fig. 8. The effect of conditioning depolarizations on the peak amplitude of test 200 mM-K^+ contractures. Each pair of records was obtained from one preparation and shows K^+ contractures in control solutions and with ClO_4^-. *A* and *B*, 10 min conditioning depolarizations in 30 mM-K^+, 10 mM-ClO_4^-. *C* and *D*, 10 min conditioning depolarizations in 40 mM-K^+, 10 mM-ClO_4^-. *E* and *F*, 5 min conditioning depolarizations in 60 mM-K^+, 2 mM-ClO_4^-. The dashed lines indicate the period of exposure to conditioning solutions and to ClO_4^-. The vertical lines show application of the test 200 mM-K^+ solution. Twitches, tetanic contractions and K^+ contractures are as described for Fig 2. t_i was measured as the increase in tension above the conditioning tension. Horizontal calibration, 5 min. Vertical calibration, 6 mN for *A* and *B*, 4 mN for *C* and *D*, 10 mN for *E* and *F*.

(Fig. 8). The depression of test 200 mM-K^+ contractures in ClO_4^- was not due to 'run-down' (Dulhunty, 1991) since it was also seen in the average data in Fig. 9, where the normal test tension was calculated from the mean T_i obtained before, and after, the ClO_4^- experiment. The inactivation curves in Fig. 9 were shifted by 4–6 mV to more negative potentials in ClO_4^- (Table 7).

The rate at which test tension fell to a steady-state level was not altered by ClO_4^-. Normally the peak amplitude of test 200 mM-K^+ contractures falls rapidly during the first 3 min of conditioning depolarization and then falls slowly between 3 and 10 min (Dulhunty, 1991). There was a $-1{\cdot}3$ mV shift in V_i between 3 and 5 min in 2 mM-ClO_4^- which was similar to the -2.1 mV shift in the control curve (Table 7).

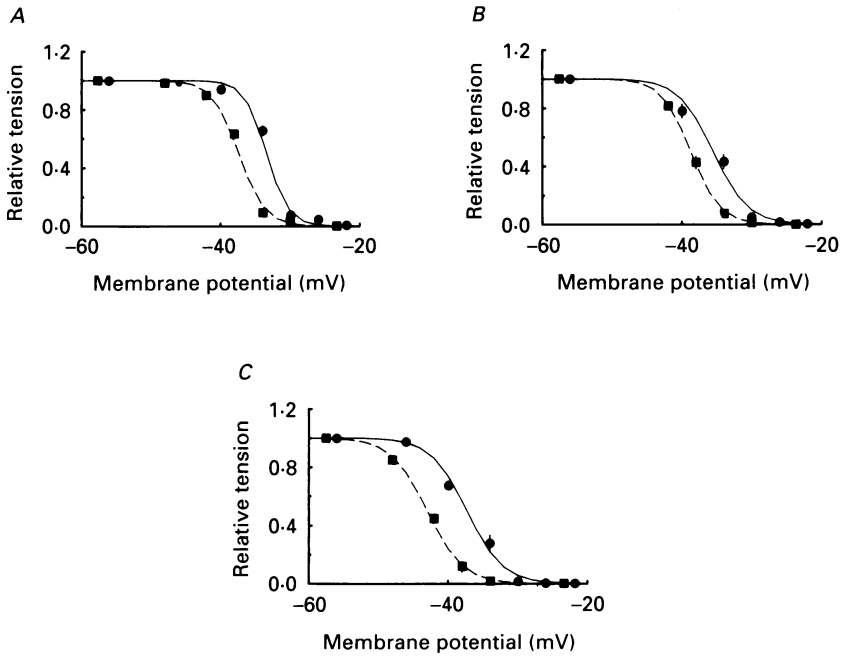

Fig. 9. Inactivation of test 200 mM-K^+ contracture tension. Relative peak amplitude of test 200 mM-K^+ contractures, T_i, is plotted against the membrane potential in conditioning high-K^+ solutions. The symbols show average T_i, for at least five preparations, in control solutions (●) and in ClO_4^- (■). The vertical bars show ±S.E.M. where this exceeds the dimensions of the symbols. *A*, 3 min conditioning, 2 mM-ClO_4^-. *B*, 5 min conditioning, 2 mM-ClO_4^-. *C*, 10 min conditioning, 10 mM-ClO_4^-. The curves show the best, least-squares fit of eqn (5) to the data. Continuous lines, curves fitted to control data; dashed lines, curves fitted to ClO_4^- data.

TABLE 7. Effects of ClO_4^- on V_i and k, obtained from the best, least-squares fit of eqn (5) to the average, normalized test 200 mM-K^+ contracture data

	T_{max}	V_a (mV)	k (mV)
3 min inactivation			
Control	1·00	−33·4	1·6
2 mM-ClO_4^-	1·00	−37·4	1·9
5 min inactivation			
Control	1·00	−35·5	2·5
2 mM-ClO_4^-	1·00	−38·7	2·1
10 min inactivation			
Control	1·00	−37·5	2·6
10 mM-ClO_4^-	1·00	−43·0	2·6

Repriming of K^+ contracture tension

The shift in the inactivation curves (Fig. 9) could mean either that ClO_4^- induced a new, more strongly inactivated state or that, for a given V_m, a greater fraction of the voltage sensor was trapped in existing inactive conformations. Induction of a

more strongly inactivated state prolongs the time required for the system to recover upon repolarization (Luttgau *et al.* 1986; Caputo & Bolanos, 1990).

Twitches often recovered more rapidly from inactivation in ClO_4^- (Fig. 10*A*). On average, times taken for the tetanus to reach 90% of its final value following

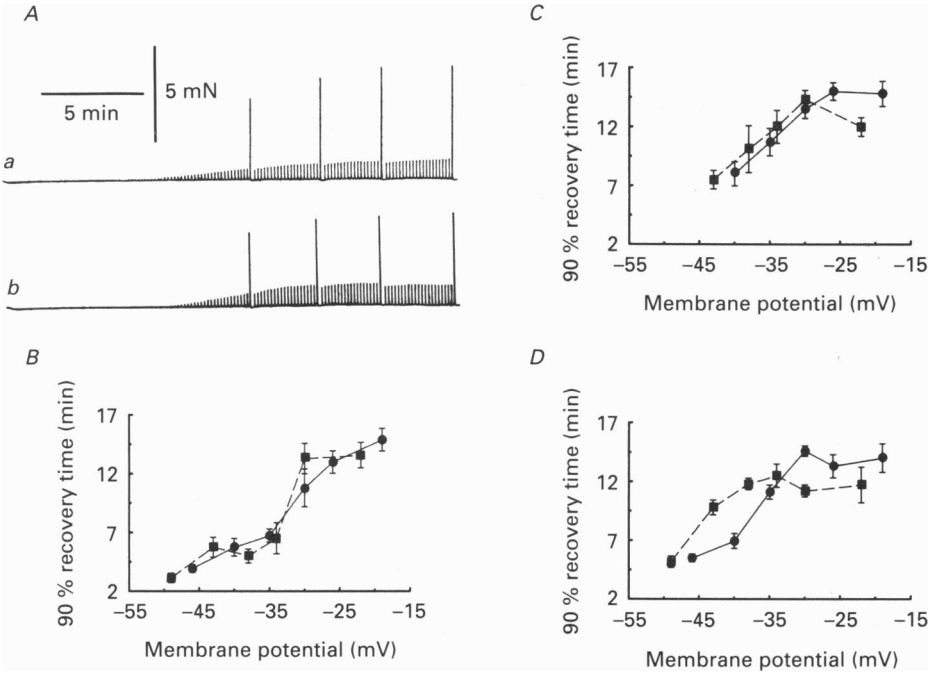

Fig. 10. Repriming during repolarization after prolonged depolarization. *A*, examples of twitch and tetanic contractions during recovery from 5 min in 120 mM-K^+ in control solutions (*a*) or in 2 mM-ClO_4^- (*b*). Each record starts when the fibres were repolarized in 3·5 mM-K^+. Calibrations: horizontal, 5 min; vertical, 5 mN. *B*, *C* and *D* show average times for tetanic tension to recover to 90% of its final value plotted against membrane potential in conditioning high-K^+ solutions. ●——●, recovery from control depolarization. ■---■, recovery from depolarization in ClO_4^-. Each symbol represents the average of at least five observations. *A*, after 3 min conditioning, 2 mM-ClO_4^-. *B*, after 5 min conditioning, 2 mM-ClO_4^-. *C*, after 10 min conditioning, 10 mM-ClO_4^-. The vertical bars show ±1 S.E.M. where this exceeds the dimensions of the symbol.

inactivation in ClO_4^- were similar to, or faster than, control times (Fig. 10*B*, *C* and *D*). Thus the negative shift in V_i was due to conversion of a larger fraction of the voltage sensor to the inactive states.

The mechanism of ClO_4^- contractures

ClO_4^- contractures were seen in fifty-four out of seventy-two preparations in 2 mM-ClO_4^- and in thirty out of thirty-two preparations in 10 mM-ClO_4^-. Contractures in 2 and 10 mM-ClO_4^- achieved, respectively, 2·6±0·2% and 5·7±0·5% of maximum tension. Tension was too small to measure in 0·5 mM-ClO_4^-. The contractures

developed at the same time as the increase in twitch tensions (Figs 11 and 12), suggesting that the underlying mechanism was located in the T-tubules. Unlike contractures described in skinned fibres (Fill & Best, 1990), tension in these ClO_4^- contractures did not inactivate.

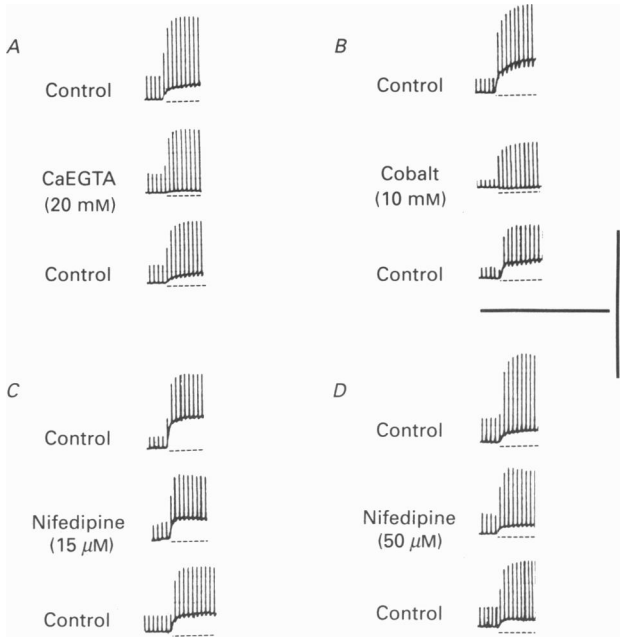

Fig. 11. ClO_4^- contractures with superimposed twitches. The dashed lines indicate exposure to ClO_4^-. Each triplet of records shows, from the top: a contracture in 10 mM-ClO_4^- in standard control solution; a contracture in test solution plus 10 mM-ClO_4^- after 10–15 min equilibration in the test solution alone; a contracture in 10 mM-ClO_4^- following 10–15 min recovery in control solutions. The test solutions were: *A*, solution A (Table 1); *B*, solution C (Table 1); *C* and *D*, 15 or 50 μM-nifedipine in the standard control solution. Horizontal calibration, 5 min. Vertical calibration, 4 mN for *A* and *B*, 6 mN for *C* and 5 mN for *D*.

The mechanism of the ClO_4^- contracture was not clear. ClO_4^- did not depolarize the fibres (Fig. 2) and the contracture could not be attributed to the negative shift in activation, since contraction threshold was at least 20 mV more positive than the resting membrane potential with 10 mM-ClO_4^- (Fig. 4). Fibres with potentials around −50 mV might have been activated by ClO_4^-. However, preparations were rejected when the ratio of 200 mM-K^+ contracture to tetanic tension was larger than 1·2 (fibres at −50 mV generate K^+ contractures (Fig. 9), but inactivation of Na^+ channels (Ruff, Simoncini & Stuhmer, 1988) prevents action potentials). Similar peak tetanic and 200 mM-K^+ contracture tensions can be seen in fibres generating strong ClO_4^- contractures in Fig. 3.

The mechanism of the ClO_4^- contracture was investigated using solutions listed in Table 1. The rationale for the procedures is outlined above in the section exploring the nature of the slow decay of K^+ contracture tension in ClO_4^-.

Contribution of external Ca^{2+}

Contractures in 10 mM-ClO_4^- were reversibly blocked in two bundles of fibres (Fig. 11*A*) when external $CaSO_4$ was replaced by $MgSO_4$, and in four bundles when $CaSO_4$ was replaced by $CoSO_4$ (Fig. 11*B*). Contractures were not blocked by 15 μM ($n = 3$),

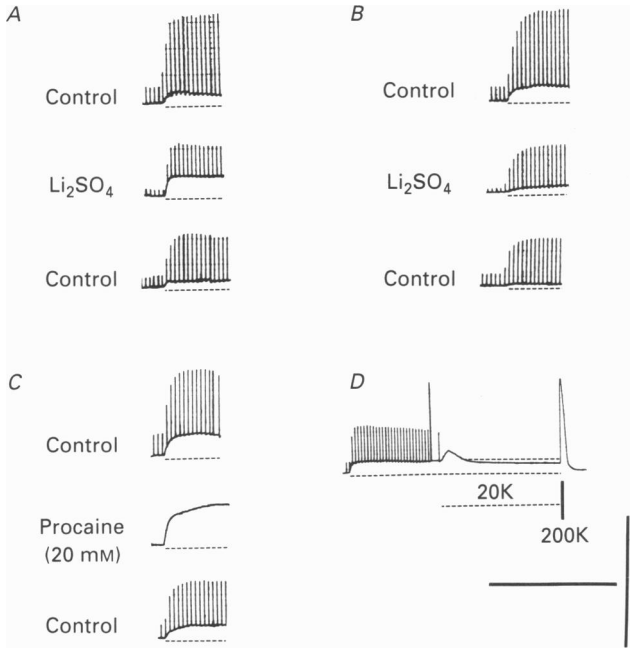

Fig. 12. The effect of external Na^+, procaine and depolarization on ClO_4^- contractures. The format for the triplets of records in *A*, *B* and *C* is the same as that in Fig. 11. Test solutions were: *A*, solution F (Table 1); *B*, solution G, (Table 1); *C*, 20 mM-procaine added to standard control solutions. *D* shows a 10 mM-ClO_4^- contracture with superimposed twitches, tetanus and 20 mM-K^+ contracture. The upper dashed line indicates the level of ClO_4^- contracture prior to the 20 mM-K^+ contracture. The dashed line immediately below the record indicates the addition of ClO_4^- and the lower dashed line indicates addition of 20 mM-K^+. Horizontal calibration, 5 min for *A*, *B*, and *C*, 7 min for *D*. Vertical calibration, 8 mN for *A*, 6 mN for *B*, 8 mN for *C*, 10 mN for *D*.

Fig. 11*C*) or 50 μM ($n = 2$, Fig. 11*D*) nifedipine. Therefore the increase in tension depended on external Ca^{2+}, but not on Ca^{2+} influx through voltage-dependent, dihydropyridine-sensitive channels.

Contribution of Na^+–Ca^+ exchange and $InsP_3$

An increase in internal Ca^{2+} and contraction would occur if ClO_4^- stimulated the Ca^{2+}–Ca^{2+} exchange mode of Na^+–Ca^{2+} exchange. Contractures were potentiated in one preparation when 80% of the Na^+ was replaced by Li^+ (Fig. 12*A*), and depressed in two others when all Na^+ was replaced (Fig. 12*B*). The inconsistent effect of Li^+ suggested (a) that the contracture did not depend on the Ca^{2+}–Ca^{2+} exchange and (b) that $InsP_3$ was not involved.

Further evidence against an $InsP_3$ effect was the reduction in contractures when one bundle of fibres was depolarized to −62 mV in 10 mM-K^+ prior to addition of ClO_4^-: $InsP_3$ is more effective in depolarized fibres (Donaldson, Goldberg, Walseth & Huetteman, 1988).

Contribution of Ca^{2+}-activated Ca^{2+} release

Procaine depresses Ca^{2+}-activated Ca^{2+} release in skinned fibres (Donaldson, 1986) and was used to determine whether a ClO_4^--stimulated influx of external Ca^{2+} produced contraction by inducing further Ca^{2+} release from the sarcoplasmic reticulum. ClO_4^- contractures were significantly larger than normal in 10 and 20 mM-procaine (Fig. 11*C*) indicating that Ca^{2+} activation of Ca^{2+} release was not involved in the ClO_4^- contracture.

ClO_4^- contractures are depressed during K^+ contractures

Inactivation of K^+ contractures in ClO_4^- often reduced tension to a level below that of the preceding ClO_4^- contracture (Fig. 12*D*). The initial hypothesis was that ClO_4^- contractures were influenced by voltage-dependent inactivation of E–C coupling. An alternative explanation was that the mechanism generating the ClO_4^- contracture has a negative voltage sensitivity. This was supported by the reduced amplitude of ClO_4^- contractures following depolarization in 10 mM-K^+ (described above).

DISCUSSION

The action of ClO_4^- on rat soleus fibres differed from that reported for amphibia (Gomolla *et al.* 1983) in that (a) there were significant changes in the decay of K^+ contracture tension and in the voltage dependence of inactivation and (b) a contracture developed at the resting membrane potential.

The 'hyperslow' decay of K^+ contracture tension in ClO_4^-

The decay of K^+ contractures during steady depolarization in rat soleus fibres is normally an order of magnitude slower than in amphibia (Dulhunty, 1991) where an 'ultraslow' inactivation process, lasting 100 s has been described (Caputo & Bolanos, 1990). The induction by 10 mM-ClO_4^- of a component of the K^+ contracture whose decay continued for 10 min was remarkable. The possibility that tension was maintained by Ca^{2+} influx across the surface membrane, or a slow secondary mechanism, was excluded.

The slow decay of tension in ClO_4^- followed the time course of the 'hyperslow' reduction in peak test 200 mM-K^+ contracture amplitude during depolarization of soleus fibres which possibly reflects the transition of the voltage sensor to a second inactivated state (Dulhunty, 1991). Evidence for the transition to the second inactivated state has not previously been described in the decay of K^+ contractures.

Action of ClO_4^- on the voltage sensor

The results can be explained solely by an action of ClO_4^- on the voltage-sensitive molecule. It is generally assumed that depolarization converts a fraction of voltage-sensitive molecules from a precursor state to an active state and then to inactive

states (Chandler *et al.* 1976; Luttgau *et al.* 1986; Dulhunty & Gage, 1988). The only action of ClO_4^- in frog fibres is thought to be an increase in the fraction of voltage-sensitive molecules that are converted to the active state upon depolarization: there are similar shifts to the left in the activation curves for tension and asymmetric charge movement (Luttgau *et al.* 1983; Huang, 1986; Csernoch *et al.* 1987).

We suggest that the major action of ClO_4^- is also on the voltage-sensitive molecule in mammals. The results could be simply explained if the slow inactivation step is normally not seen in the decay of K^+ contracture tension because $[Ca^{2+}]$ falls below contraction threshold. The amount of the voltage sensor converted to the active state is substantially increased in the presence of ClO_4^- and $[Ca^{2+}]$ remains above the threshold for contraction during slow inactivation. A slow step in the decay of K^+ contracture tension in ClO_4^- may also be seen in amphibian fibres with careful examination of inactivation.

The mechanism underlying ClO_4^- contractures

The contracture induced by ClO_4^- clearly depended on external Ca^{2+}, but not on Ca^{2+} influx through dihydropyridine-sensitive Ca^{2+} channels or Na^+–Ca^{2+} exchange. Neither Ca^{2+} activation of Ca^{2+} release or InsP_3 were involved. It is suggested that Ca^{2+} enters the fibres through ion channels in the surface membrane that are open at the resting V_m. A divalent cation channel, open at the resting membrane potential, has been described in cardiac muscle (Rosenberg, Hess & Tsien, 1988; Coulombe, Lefevre, Baro & Coraboeuf, 1989). The open probability of this channel is greatest at -70 to -80 mV and declines at more positive, or more negative, membrane potentials. A similar channel has been described in myotubes of human or mouse origin (Fong, Turner, Denetclaw & Steinhardt, 1990). The negative voltage sensitivity of this channel would account for the decline in ClO_4^- contracture tension with depolarization.

Tension during the ClO_4^- contracture did not depend on Ca^{2+}-activated Ca^{2+} release. Therefore Ca^{2+} entering from the outside produced tension either by direct activation of the contractile proteins or activation of a procaine-insensitive component of calcium release (Donaldson, 1986).

We thank Professor P. W. Gage and Dr P. Junankar for their helpful comments on the manuscript and Mrs S. Curtis for technical assistance.

REFERENCES

ADRIAN, R. H., CHANDLER, W. K. & HODGKIN, A. L. (1969). The kinetics of mechanical activation in frog muscle. *Journal of Physiology* **204**, 207–230.

ALMERS, W., MCCLESKEY, E. W. & PALADE, P. T. (1985). Calcium channels in vertebrate skeletal muscle. In *Calcium in Biological Systems*, ed. RUBIN, R. P., WEISS, G. B. & PUTNEY, J. W., pp. 321–329. Plenum Publishing Corp., New York.

BAKER, P. F., BLAUSTEIN, M. P., HODGKIN, A. L. & STEINHARDT, R. A. (1967). The effect of sodium concentration on calcium movements in giant axons of *Loligo forbesi*. *Journal of Physiology* **192**, 43-44*P*.

BERRIDGE, M. J. & IRVINE, R. F. (1989). Inositol phosphates and cell signalling. *Nature* **341**, 197–204.

BERWE, D., GOTTSCHALK, G. & LUTTGAU, H. CH. (1987). Effects of the calcium antagonist gallopamil (D600), upon excitation–contraction coupling in toe muscle fibres of the frog. *Journal of Physiology* **385**, 693–707.

BLAUSTEIN, M. P. & HODGKIN, A. L. (1969). The effect of cyanide on the efflux of calcium from squid axons. *Journal of Physiology* **200**, 497–527.

CAPUTO, C. & BOLANOS, P. (1990). Ultraslow contractile inactivation in frog skeletal muscle fibers. *Journal of General Physiology* **96**, 47–56.

CHANDLER, W. K., RAKOWSKI, R. F. & SCHNEIDER, M. F. (1976). Effects of glycerol treatment and maintained depolarization on charge movement in skeletal muscle. *Journal of Physiology* **254**, 285–316.

CHUA, M. & DULHUNTY, A. F. (1988). Inactivation of excitation–contraction coupling in rat extensor digitorum longus and soleus muscles. *Journal of General Physiology* **91**, 737–757.

COSTANTIN, L. L, (1974). Contractile activation in frog skeletal muscle. *Journal of General Physiology* **63**, 657–674.

COULOMBE, A., LEFEVRE, I. A., BARO, I. & CORABOEUF, E. (1989). Barium- and calcium-permeable channels open at negative membrane potentials in rat ventricular myocytes. *Journal of Membrane Biology* **111**, 57–67.

CSERNOCH, L., KOVACS, L. & SZUCS, G. (1987). Perchlorate and the relationship between charge movement and contractile activation in frog skeletal muscle fibres. *Journal of Physiology* **390**, 213–227.

CURTIS, B. A. (1988). Na/Ca exchange and excitation–contraction coupling in frog fast fibres. *Journal of Muscle Research and Cell Motility* **9**, 415–427.

DONALDSON, S. K. (1986). Mammalian muscle fiber types: Comparison of excitation–contraction coupling mechanisms. *Acta Physiologica Scandinavica* **128**, suppl. 556, 157–165.

DONALDSON, S. K., GOLDBERG, N. D., WALSETH, T. F. & HUETTEMAN, D. A, (1988). Voltage dependence of inositol 1,4,5-trisphosphate-induced Ca^{++} release in peeled skeletal muscle fibers. *Proceedings of the National Academy of Sciences of the USA* **85**, 5749–5753.

DULHUNTY, A. F. (1979). Distribution of potassium and chloride permeability over the surface and T-tubule membranes of mammalian skeletal muscle. *Journal of Membrane Biology* **45**, 293–310.

DULHUNTY, A. F. (1991). Activation and inactivation of excitation–contraction coupling in rat soleus muscle. *Journal of Physiology* **439**, 605–626.

DULHUNTY, A. F. & GAGE, P. W. (1985). Excitation–contraction coupling and charge movement in denervated rat extensor digitorum longus and soleus muscles. *Journal of Physiology* **358**, 75–89.

DULHUNTY, A. F. & GAGE, P. W. (1988). Effects of extracellular calcium concentration and dihydropyridines on contraction in mammalian skeletal muscle. *Journal of Physiology* **399**, 63–80.

FILL, M. & BEST, P. M. (1990). Effect of perchlorate on calcium release in skinned fibres stimulated by ionic substitution and caffeine. *Pflügers Archiv* **415**, 688–692.

FONG, P., TURNER, P. R., DENETCLAW, W. F. & STEINHARDT, R. A. (1990). Increased activity of calcium leak channels in myotubes of Duchenne human and mdx mouse origin. *Science* **250**, 673–676.

FOULKS, J. G., MILLER, J. A. D. & PERRY, F. A. (1973). Repolarization-induced reactivation of contracture tension in frog skeletal muscle. *Canadian Journal of Physiology and Pharmacology* **51**, 324–334.

FOULKS, J. G. & PERRY, F. A. (1979). The effects of temperature, local anaesthetics, pH, divalent cations, and group-specific reagents on repriming and repolarization-induced contractures in frog skeletal muscle. *Canadian Journal of Physiology and Pharmacology* **57**, 619–630.

GOMOLLA, M., GOTTSCHALK, G. & LUTTGAU, H. CH. (1983). Perchlorate-induced alterations in electrical and mechanical parameters of frog skeletal muscle fibres. *Journal of Physiology* **343**, 197–214.

HODGKIN, A. L. & HOROWICZ, P. (1960). Potassium contractures in single muscle fibres. *Journal of Physiology* **153**, 386–403.

HUANG, C. L.-H. (1986). The differential effects of twitch potentiators on charge movement in frog skeletal muscle. *Journal of Physiology* **380**, 17–33.

LUTTGAU, H. C., GOTTSCHALK, G., KOVACS, L. & FUXREITER, M. (1983). How perchlorate improves excitation–contraction coupling in skeletal muscle fibers. *Biophysical Journal* **43**, 247–249.

LUTTGAU, H. CH. (1963). The action of calcium ions on potassium contractures of single muscle fibres. *Journal of Physiology* **168**, 679–697.

LUTTGAU, H. CH., GOTTSCHALK, G. & BERWE, D. (1986). The role of Ca^{++} in activation and paralysis of excitation–contraction coupling in skeletal muscle. *Fortschritte der Zoologie* **33**, 195–203.

MCLAUGHLIN, S., BRUDER, A., CHEN, S. & MOSER, C. (1975). Chaotropic anions and the surface potential of bilayer membranes. *Biochimica et Biophysica Acta* **394**, 304–313.

NOIREAUD, J. & LEOTY, C. (1988). Effect of external sodium substitution on potassium contractures of mammalian muscles: possible involvement of sarcolemma-bound calcium and Na^{+}–Ca^{2+} exchange. *Quarterly Journal of Experimental Physiology* **73**, 233–236.

PHILIPSON, K. D. (1985). Sodium–calcium exchange in plasma membrane vesicles. *Annual Reviews of Physiology* **47**, 561–571.

ROSENBERG, R. L., HESS, P. & TSIEN, R. W. (1988). Cardiac calcium channels in planar lipid bilayers. *Journal of General Physiology* **92**, 27–54.

RUFF, R. L., SIMONCINI, L. & STUHMER, W. (1988). Slow sodium channel inactivation in mammalian muscle: a possible role in regulating excitability. *Muscle and Nerve* **11**, 502–510.

SIRI, L. N., SANCHEZ, J. A. & STEFANI, E. (1980). Effect of glycerol treatment on the calcium current of frog skeletal muscle. *Journal of Physiology* **305**, 87–96.

VERGARA, J., TSIEN, R. Y. & DELAY, M. (1985). Inositol 1,4,5-trisphosphate: A possible chemical link in excitation–contraction coupling in muscle. *Proceedings of the National Academy of Sciences of the USA* **82**, 6352–6356.

VOLPE, P., SALVIATI, G., DI VIRGILIO, F. & POZZAN, T. (1985). Inositol 1,4,5-trisphosphate induces calcium release from sarcoplasmic reticulum of skeletal muscle. *Nature* **316**, 347–349.